



Design and fabrication of light weight current collectors for direct methanol fuel cells using the micro-electro mechanical system technique

Min-Feng Sung^a, Yean-Der Kuan^{b,*}, Bing-Xian Chen^b, Shi-Min Lee^c

^a Department of Mechanical and Electro-Mechanical Engineering, Tamkang University, 251 Tamsui, Taiwan

^b Department of Refrigeration, Air-Conditioning and Energy Engineering, National Chin-Yi University of Technology, 411 Taichung, Taiwan

^c Department of Aerospace Engineering, Tamkang University, 251 Tamsui, Taiwan

ARTICLE INFO

Article history:

Received 12 January 2011

Received in revised form 25 February 2011

Accepted 28 February 2011

Available online 6 March 2011

Keywords:

Direct methanol fuel cell
Thermal evaporation
Micro-electro mechanical system
Current collector

ABSTRACT

The direct methanol fuel cell (DMFC) is suitable for portable applications. Therefore, a light weight and small size is desirable. The main objective of this paper is to design and fabricate a light weight current collector for DMFC usage. The light weight current collector mainly consists of a substrate with two thin film metal layers. The substrate of the current collector is an FR4 epoxy plate. The thin film metal layers are accomplished by the thermo coater technique to coat metal powders onto the substrate surfaces. The developed light weight current collectors are further assembled to a single cell DMFC test fixture to measure the cell performance. The results show that the proposed current collectors could even be applied to DMFCs because they are light, thin and low cost and have potential for mass production.

© 2011 Elsevier B.V. All rights reserved.

1. Introduction

A fuel cell is an electrical power generator that converts the chemical energy stored in fuel into electricity directly via the electrochemical reactions without moving heavily parts. For portable applications, the direct methanol fuel cell is one of the most prominent candidates to replace the lithium-ion battery because it has some specific advantages. It operates at near room temperature, is easy to store the fuel and quick to refill it, and convenient to carry and is safe. The system is easy to use, and the energy of the fuel is higher [1]. The bipolar plates are the major part of the proton exchange membrane fuel cell (PEMFC) stack in terms of weight, volume, and cost. The cost, weight, manufacturability and capability for mass production are important for the material and fabrication of the bipolar plates [2,3]. Traditionally, the bipolar plates have been constructed of graphite material. Although graphite is electrically conductive and resistant to corrosion in the fuel cell environment, it is brittle, expensive, bulky, and difficult to machine [4]. Therefore, many researchers are devoted to the development of bipolar plates and current collectors due to the aspects of materials, fabrication, processing, and geometry.

The carbon/carbon composites bipolar plates are developed using carbon powder, and the bipolar plate is manufactured either by hot-pressing the compound, directly by molding the com-

-pound powder or fabricated by slurry molding a chopped-fiber preform. Compared to the graphite material, a bipolar plate made of carbon/carbon composites has lower manufacturing cost, higher mechanical strength, good chemical stability in the cell environment, good gas tightness, light weight and maintains a high surface and bulk electronic conductivity. However, carbon/carbon composites are still not expected to achieve ambitious cost price targets because they require expensive post processing [3,5,6]. Metal-based or carbon-based polymer composites are alternative materials for bipolar plates, which have the characteristics of light weight, stable chemical resistance, strong rigidity, good electrical conductivity, inexpensive material and economical processing, and the ability to be molded into any shape and size [3,7]. Because graphite and its composites are brittle, permeable to gases/liquid, and not cost effective for high volume manufacturing processes relative to metals, metallic bipolar plates have received considerable attention in recent years for their higher mechanical strength, better durability to shock and vibrate, lack of permeability, superior manufacturability, and cost effectiveness. The main handicap of metals is the lack of corrosion resistance in the harsh, acidic and humid environment inside fuel cells. Therefore, many attempts have been made to improve the corrosion resistance without sacrificing surface contact resistance but while maintaining cost effectiveness, such as using noble metals, stainless steel, copper alloy, metal surfaces coated with nitride or carbide-based alloys, titanium with FC5 coated and gold-coated titanium and niobium [8–14]. Printed circuit board (PCB) technology, a well-known and low cost process, has been applied to fabricate planar fuel cells.

* Corresponding author. Tel.: +886 4 23924505x8256; fax: +886 4 23932758.
E-mail addresses: ydkuan@ncut.edu.tw, c699611@yahoo.com (Y.-D. Kuan).

The main advantage of PCB fuel cells is that the electric circuits can be integrated on the PCB and the energy management system EMS, and that a dc–dc converter can be embedded into the PCB fuel cell module. However, MEAs might be degraded throughout the PCB process [15–20]. The effect of the free open ratio and total perimeter length of the current collectors for the planar DMFC have also been investigated [21,22]. Several research groups adopted the PCB technology to make segmented cells. The segmented cells technique was focused on the development of diagnostic tools, which can be combined with electrochemical methods to provide direct information on the local current density distribution of the cell but also on the other phenomena occurring inside the cell under different operating conditions. This information is helpful for optimizing the fuel cell electrode, flow field and manifold designs [23–25].

The techniques of micro-electro mechanical system (MEMS) are being adopted to miniaturize DMFCs. Lu et al. [26] developed a micro DMFC by the fabrication of a silicon wafer with deposited metal layers for collecting the generated electricity. Cha et al. [27] presented all-polymer micro DMFCs using UV lithography, lift-off, and metallization processes. Yao et al. [28] developed a silicon-based micro-scale DMFC system, which contains a silicon wafer with arrays of etched holes selectively coated with a non wetting agent for collecting water at the cathode, a silicon membrane micro pump for pumping the collected water from the cathode to the anode, and a passive liquid-gas separator for CO₂ removal. Zhang et al. [29] developed and showed the visibility of a MEMS-based DMFC with nanoimprint technology. The main problem associated with silicon based micro fuel cells is the brittleness of silicon; thus, the mechanical strength may be low. Although the fragility problem can be improved by using a polymer as the substrate, the substrate is still soft. Therefore, the development of another substrate for fuel cells is a very attractive topic for micro fuel cells.

Although the PCB technique has been applied to current collectors or bipolar plates for several years, the conduction layer usually adopted copper-clad placed on the surface of the substrate and the corrosion-resistance layer further coated onto the copper clad surface by electroplating [30,31]. This paper focuses on the development of a light weight current collector using FR4/epoxy plates, a composite that is widely adopted as the substrate in print circuit boards. This paper further proposes a different method to coat the metal layers onto the substrate surface. Thermal evaporation, an MEMS technique, is adapted to coat two metal layers onto the surface such that the cost can be reduced and mass production is possible.

2. Fabrication processes of the current collectors

The fabrication processes of the current collectors include the machining to prepare the substrate of the current collectors and thermal evaporation to coat the metal films on the substrate. The detailed procedures are described below.

In the machining process, FR4 epoxy laminates were adopted as the material for the substrate of the current collectors. The geometry of the current collectors, including the outlines and opening holes, were drawn using AUTOCAD software and converted to the CNC code. A substrate plate was fixed at the working surface of a milling machine. Then, the path of the end milling tool was controlled by the CNC codes, and the outline and opening holes of the substrate were carved or drilled using the milling tool. The substrates of anode and cathode substrates of the current collectors were the same. Fig. 1 shows the geometry with the main dimensions of the substrate, and the thickness is 0.5 mm. The reactive area of the membrane electrolyte assembly (MEA) is 35 mm × 35 mm, and the free open holes are arranged around this area.

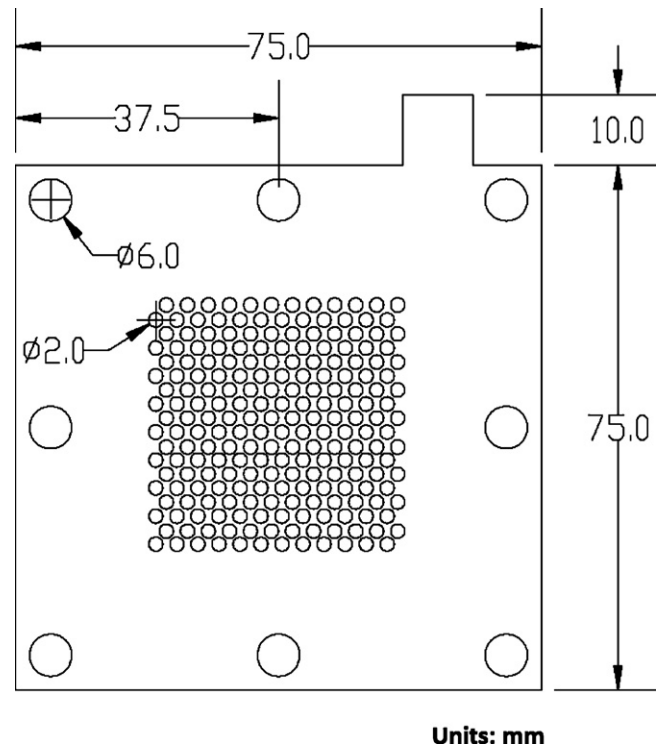


Fig. 1. The geometry and main dimensions of the substrate.

After the machining process was completed, the thermal evaporation process started, which is described as follows. There are two stages of thermal evaporation to coat two different metal thin films onto the substrate of the current collector. The first stage is to coat the first thin films as the electricity conduction layer, and the second stage is to coat the second thin films as the corrosion resistance layer. The main structure of the thermal evaporation machine is shown in Fig. 2, and the inside of the machine is shown in Fig. 3. The substrate of the current collector is held by the substrate carrier. The metal ingots that are the evaporation sources, such as copper ingots, nickel ingots, or aluminum ingots, are placed in the tungsten boat. Then, the chamber is evacuated to 5E–5 Torr, and the metal ingots of the evaporation sources are vaporized by the heat generation via the high current source going through the tungsten boat. There are two sets of the metal evaporation sources inside

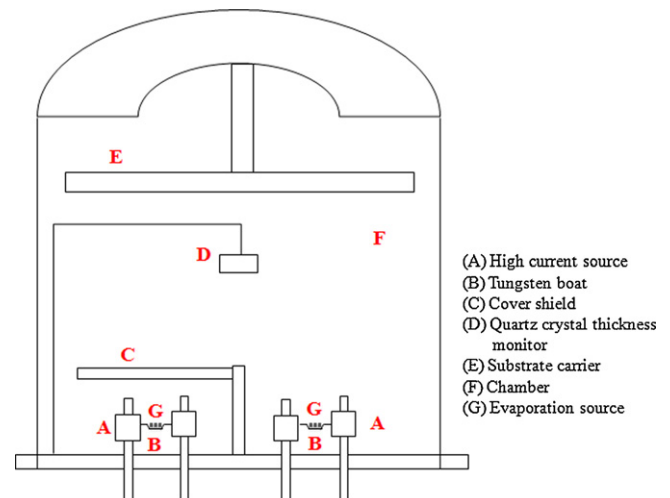


Fig. 2. The main structure of the thermal evaporation machine.

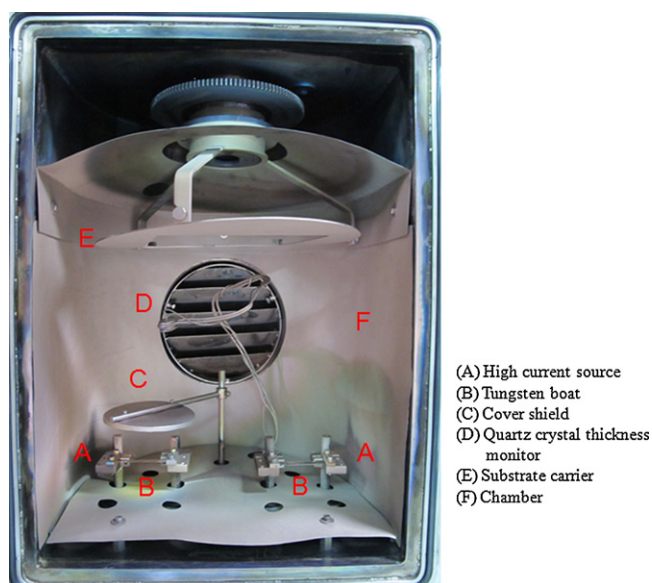


Fig. 3. The inside picture of the thermal evaporation machine.

the evaporation machine adopted in this research. The cover shield is above the tungsten boat when the metal ingots are heated and vaporized in the beginning. Once the metal ingots are well vaporized, the cover shield of the tungsten boat is removed from above, and the metal vapor is released and coated onto the surface of the substrate of the current collector. The thickness of coated metal thin films can be estimated by a quartz crystal thickness monitor. Once the thickness of the metal thin film reaches the target value, the high current source is cut off. After finishing the first stage of the thermal evaporation process, the breaking vacuum process for the chamber is executed. Then, different metal ingots are placed in the tungsten boats, and the second stage of the thermal evaporation process starts. After the second stage of the thermal evaporation process is complete, the breaking vacuum process for the chamber is executed, and the process of making the current collector is completed. Fig. 4a is a picture of the substrate of the current collector, and Fig. 4b is a picture of the finished current collector where two metal films are coated onto the substrate surface via the thermal evaporation process.

3. Results and discussion

3.1. Resistivity comparison

A good current collector of a fuel cell should have high electrical conductivity or low electrical resistivity. Therefore, to figure out the electricity conductivity of the current collectors under different metal thermal evaporation combinations, the values of resistivity at nine points, as shown in Fig. 5, were measured by a four-point probe instrument. The distances between the probes were 1 mm. Table 1 is a comparison of the resistivity values using aluminum and copper metal evaporations of 5 kÅ in thickness as the source of thermal coating for the conduction layer under the same corrosion layer of 2 kÅ in thickness. The results show that the resistivity of the current collector with an aluminum conduction layer is much higher than the one with a copper conduction layer. Therefore, using copper thermal evaporation to make the conduction layer is suggested.

Further investigation used thermal evaporation to coat different thicknesses of copper conduction layers on the substrate under the same thickness of the nickel corrosion resistance layer, and the electricity resistivity was compared and is shown in Table 2. The results show that the substrate with Cu 5 kÅ/Ni 2 kÅ thin film layers had

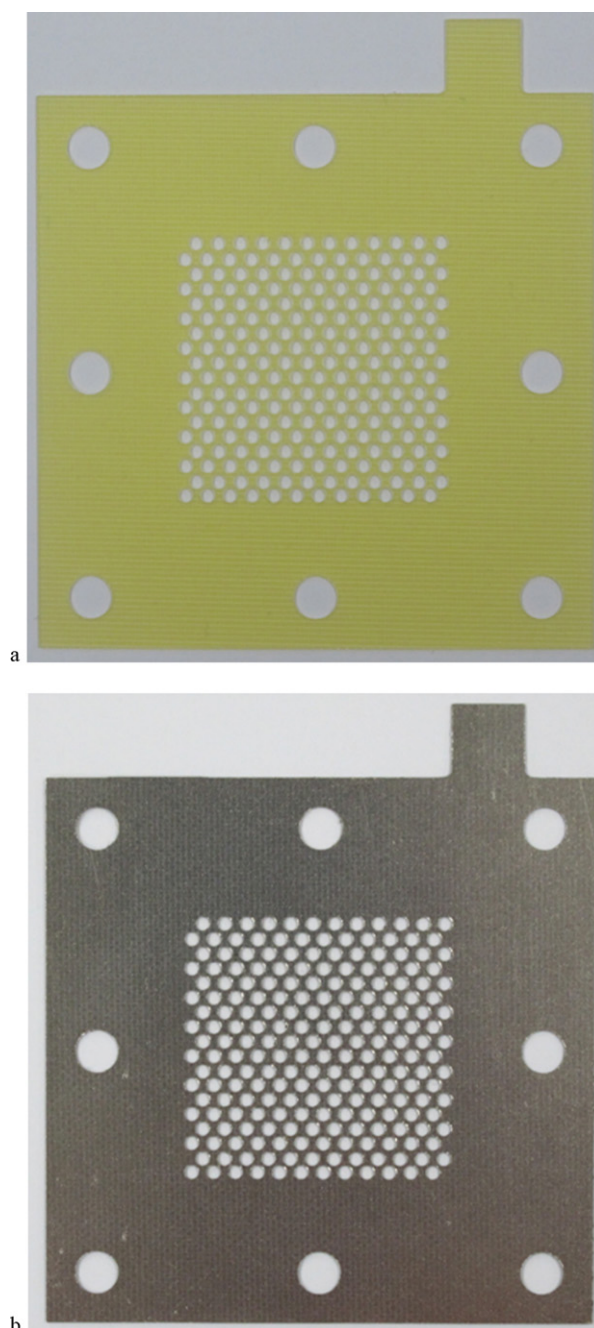


Fig. 4. Pictures of the current collector. (a) Picture of the substrate of the current collector. (b) Picture of the finished current collector after complete thermal evaporation processes.

the highest resistivity, and the average value was 12.57 mΩ. The substrate with thin films with Cu 10 kÅ/Ni 2 kÅ layers had a lower resistivity, and the average value was 6.99 mΩ. The substrate with thin films with Cu 15 kÅ/Ni 2 kÅ layers had the lowest resistivity, and the average value was 3.42 mΩ. A thicker copper conduction layer leads to a higher capability of the electric conduction.

3.2. Cell performance comparison

To evaluate the performance of DMFC with the current collectors using different thermal evaporation conditions for the substrates, the current collectors were used in a single cell DMFC test, and the polarization curves were measured. The polarization curve reflects the different limiting mechanisms occurring during the operation

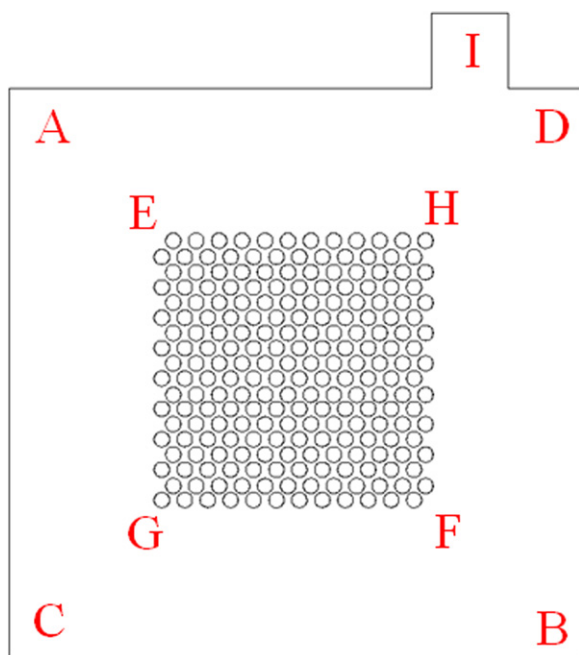


Fig. 5. The selected nine monitored points at the current collector for measuring the resistivity.

Table 1
Resistivity comparison using a 5 kÅ Al and 5 kÅ Cu thickness conduction layer under the same corrosion resistance layer.

Monitored point	Substrate with different thin films	
	Al 5 kÅ/Ni 2 kÅ	Cu 5 kÅ/Ni 2 kÅ
A	130	12.2
B	120	12.5
C	120	12.8
D	130	12.7
E	140	12.6
F	140	12.9
G	150	12.6
H	130	12.6
I	130	12.2
Average	132	12.5

Units: mΩ.

Table 2
Resistivity comparison using Al and Cu as the conduction layer.

Monitored point	Substrate with different thin films		
	Cu 5 kÅ/Ni 2 kÅ	Cu 10 kÅ/Ni 2 kÅ	Cu 15 kÅ/Ni 2 kÅ
A	12.2	6.5	3.4
B	12.5	6.9	3.9
C	12.8	7.2	3.4
D	12.7	7.1	3.1
E	12.6	7	3.2
F	12.9	7.4	3.3
G	12.6	7.5	3.5
H	12.6	6.4	3.6
I	12.2	6.9	3.4
Average	12.5	6.9	3.4

Units: mΩ.

of a fuel cell under different current density ranges [32]. A single cell DMFC test fixture was constructed, and the exploded view of the 3D drawing is shown in Fig. 6. A picture of the array of components is shown in Fig. 7. The membrane electrolyte assembly was sandwiched between the anode and cathode current collectors, and the current collectors were fabricated by the method in this paper. Both anode and cathode flow boards were made of polymethylmethacrylate (PMMA) and assembled at the two end sides. Each anode and cathode flow board was grooved with a single serpentine flow channel on it. A polytetrafluoroethylene (PTFE) gasket was placed between each of the two layers to prevent leakage. The schematic illustration of the experimental setup to measure the DMFC polarization curves is shown in Fig. 8. The DMFC was placed into an environment control chamber. A beaker containing the methanol solution, was preheated by a temperature controlled water bath. The methanol solution was pumped into the DMFC anode by a squire pump. The airflow was pumped into the DMFC cathode by an air pump with an airflow regulator. The DMFC was loaded by a DC electric loader. All the experiments were conducted at 55 °C and 60% RH in a 2 M methanol/DI water solution. The anode fuel flow rate was kept at 2 cc min⁻¹, and the cathode airflow rate was kept at 200 cc min⁻¹.

Fig. 9 shows the performance comparison of the current collectors using aluminum and copper thermal evaporations of 5 kÅ to make the conduction layer under the same corrosion resistance layer of 2 kÅ in Ni thickness. The results show that the performance of the current collector with copper conduction layer is about four times higher than the one with an aluminum conduction layer. Therefore, as mentioned in the resistivity comparison,

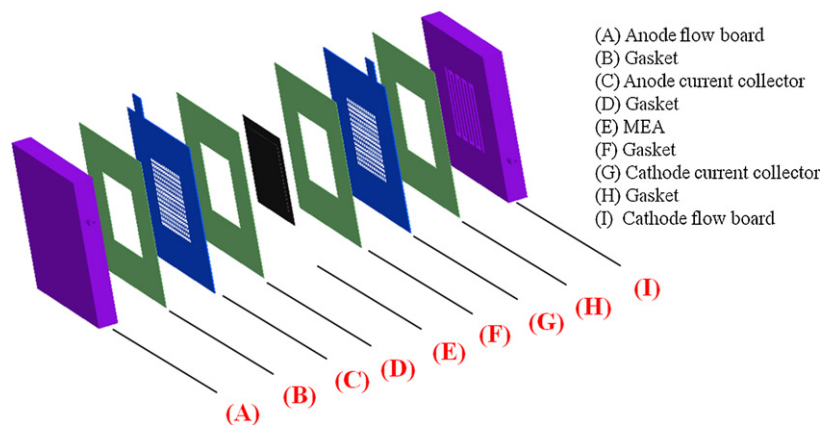


Fig. 6. Construction of the single cell DMFC test fixture; (a) anode flow board, (b) gasket, (c) anode current collector, (d) gasket, (e) MEA, (f) gasket, (g) cathode current collector, (h) gasket, and (i) cathode current collector.

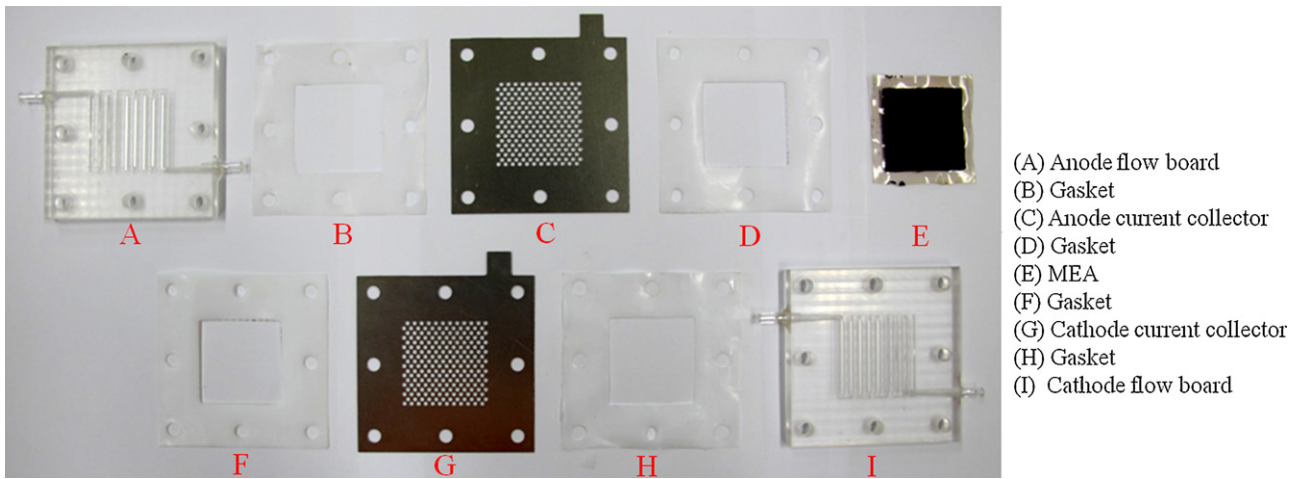


Fig. 7. The picture of the array of components of the single cell DMFC test fixture.

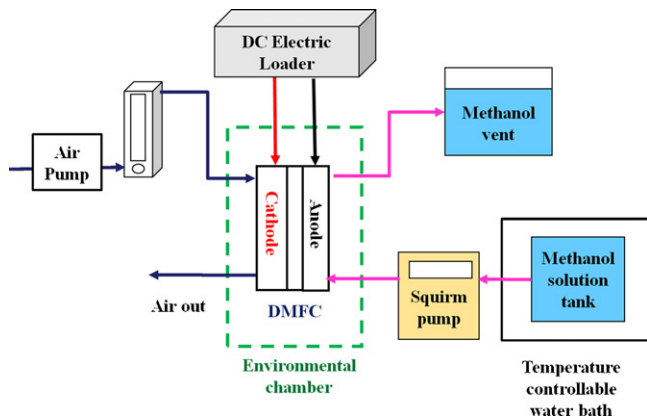


Fig. 8. Schematic illustration of the experimental setup to measure the DMFC polarization curves.

using copper thermal evaporation to make the conduction layer is suggested.

Because the copper conduction layer presents much better DMFC cell performance than the aluminum conduction layer, further investigation increased the thickness of the copper thermal evaporation layer on the substrate of the current collector from 5 kÅ and 10 kÅ, to 15 kÅ under the same Ni corrosion resistance layer of 2 kÅ. The performance comparison is shown in Fig. 10. The results

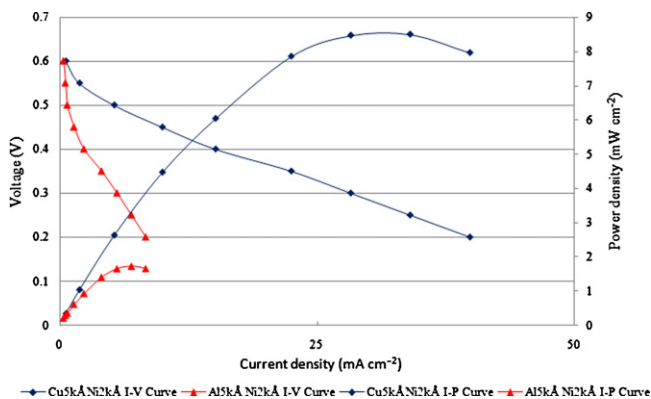


Fig. 9. Performance comparison of the DMFC with current collectors using aluminum and copper thermal evaporations of 5 kÅ thickness as the conduction layer under the same corrosion resistance layer condition of 2 kÅ Ni thickness.

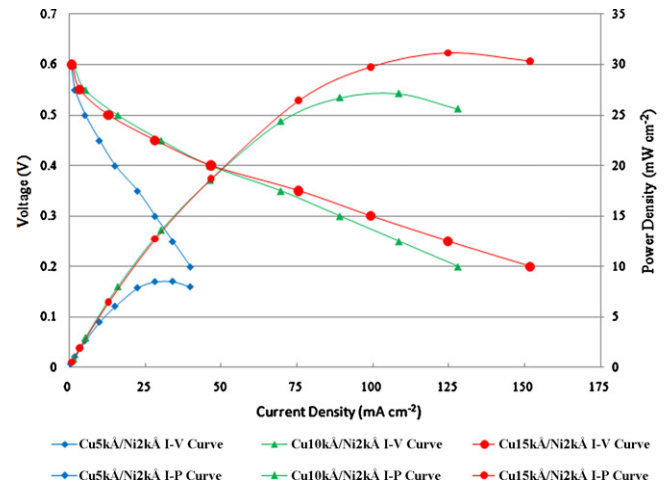


Fig. 10. Performance comparison of the DMFC with current collectors using copper thermal evaporations of different thicknesses as the conduction layer under the same corrosion resistance layer condition of 2 kÅ thickness.

show that the DMFC cell performance significantly increases with the thickness of the copper conduction layer from 5 kÅ to 10 kÅ. By further increasing the copper conduction layer thickness from 10 kÅ to 15 kÅ, the DMFC cell performance also increases. In order to ensure the usability of the developed current collectors, the stability running test was conducted under 0.3V operation voltage

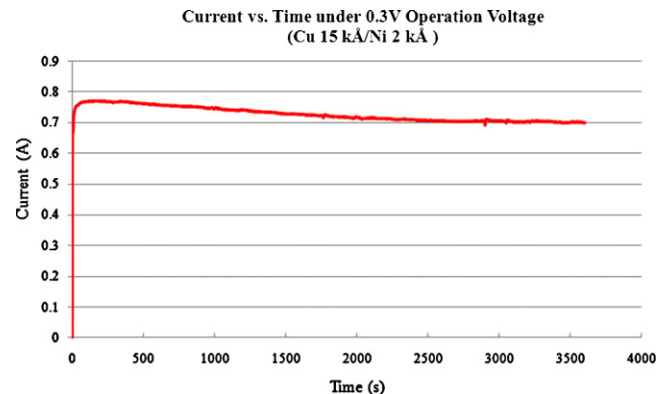


Fig. 11. Running test for the DMFC at 0.3V load for the current collector substrate with thin films with Cu 15 kÅ/Ni 2 kÅ layers.

for the current collector substrate with thin films with Cu 15 kÅ/Ni 2 kÅ layers. The output current vs. time for the DMFC is shown in Fig. 11. The results showed that the DMFC stability using the developed current collector is quite good. Therefore, these light weight current collectors can be applied to DMFC applications.

4. Conclusions

This paper presents a type of light weight current collector using thermal evaporation, which is a widely used technique in MEMS. The construction of each current collector included an FR4/epoxy plate as the substrate, which was coated with an electric conduction layer and a corrosion resistance layer via metal thermal evaporations. The Ni ingots were adopted as the source of the metal evaporation process to coat the 2 kÅ thin films as the corrosion resistance layer. Two metals, Cu and Al, were chosen as the candidates for the material of the electric conduction layer. The experimental results show that using Cu ingots as the source for metal evaporation to make the electric conduction layer presents much higher DMFC cell performance than using Al ingots. Therefore, adopting Cu ingots to make the electric conduction layer is suggested. In addition, when the Cu thin film thickness increases from 5 kÅ to 10 kÅ, the DMFC cell performance also increases significantly. With a further increase in the Cu thin film thickness from 10 kÅ to 15 kÅ, the DMFC cell performance still increases but not as much. The developed light weight current collectors were successfully demonstrated to be applied to DMFCs with full potential for a variety of applications in the future.

Acknowledgement

The authors would like to acknowledge financial support from the National Science Council of Taiwan, R.O.C. (NSC97-2221-E-167-010 and NSC 98-2221-E-167-024) and the National Nano Device Laboratories of Taiwan, R.O.C. (NDL99-C06M2G-063).

References

[1] J. Larminie, A. Dicks, *Fuel Cell Systems Explained*, 2nd ed., John Wiley & Sons Ltd., England, 2003.

- [2] V. Mehta, J.S. Cooper, *J. Power Sources* 114 (2003) 32–53.
 [3] E. Middelmann, W. Kout, B. Vogelaar, J. Lenssen, E. de Waal, *J. Power Sources* 118 (2003) 44–46.
 [4] P.L. Hentall, J.B. Lakeman, G.O. Mepsted, P.L. Adcock, J.M. Moore, *J. Power Sources* 80 (1999) 235–241.
 [5] T.M. Besmann, J.W. Klett, J.J. Henry Jr., E. Lara-Curzio, *J. Electrochem. Soc.* 147–11 (2000) 4083–4086.
 [6] E.A. Cho, U.-S. Jeon, H.Y. Ha, S.-A. Hong, I.-H. Oh, *J. Power Sources* 125 (2004) 178–182.
 [7] A. Hermann, T. Chaudhuri, P. Spagnol, *Int. J. Hydrogen Energy* 30 (2005) 1297–1302.
 [8] H. Tawfik, Y. Hung, D. Mahajan, *J. Power Sources* 163 (2007) 755–767.
 [9] D.P. Davies, P.L. Adcock, M. Turpin, S.J. Rowen, *J. Power Source* 86 (2000) 237–242.
 [10] D.R. Hodgson, B. May, P.L. Adcock, D.P. Davies, *J. Power Sources* 96 (2001) 233–235.
 [11] A. Kumar, R.G. Reddy, *J. Power Sources* 129 (2004) 62–67.
 [12] B.R. Padhy, R.G. Reddy, *J. Power Sources* 153 (2006) 125–129.
 [13] S.-G. Wang, J. Peng, W.-B. Lui, J.-S. Zhang, *J. Power Sources* 162 (2006) 486–491.
 [14] V.V. Nikam, R.G. Reddy, *Electrochim. Acta* 51 (2006) 6338–6345.
 [15] S.J. Lee, A. Chang-Chien, S.W. Cha, R. O'Hayre, Y.I. Park, Y. Saito, F.B. Prinz, *J. Power Sources* 112 (2002) 410–418.
 [16] R. O'Hayre, T. Fabian, S.-J. Lee, F.B. Prinz, *J. Electrochem. Soc.* 150 (2003) A430–438.
 [17] R. O'Hayre, D. Braithwaite, W. Hermann, S.-J. Lee, T. Fabian, S.-W. Cha, Y. Saito, F.B. Prinz, *J. Power Sources* 124 (2003) 459–472.
 [18] A. Schmitz, M. Traintz, S. Wagner, R. Hahn, C. Hebling, *J. Power Sources* 118 (2003) 162–171.
 [19] A. Schmitz, S. Wagner, R. Hahn, H. Uzun, C. Hebling, *J. Power Sources* 127 (2004) 197–205.
 [20] Y.-D. Kuan, C.-H. Chang, *J. Fuel Cell Sci. Technol.* 6 (2009) 011016.1–011016.9.
 [21] J.-Y. Chang, Y.-D. Kuan, S.-M. Lee, S.-R. Lee, *J. Power Sources* 184 (2008) 180–190.
 [22] Y.-D. Kuan, J.-Y. Chang, S.-M. Lee, S.-R. Lee, *J. Power Sources* 187 (2009) 112–122.
 [23] M. Schulze, E. Gülzow, St. Schönbauer, T. Knöri, R. Reissner, *J. Power Sources* 173 (2007) 19–27.
 [24] D.U. Sauer, T. Sanders, B. Frick, T. Baumhöfer, K. Wippermann, A.A. Kulikovskiy, H. Schmitz, J. Mergel, *J. Power Sources* 176 (2008) 477–483.
 [25] J. Wu, X.Z. Yuan, H. Wang, M. Blanco, J.J. Martina, J. Zhang, *Int. J. Hydrogen Energy* 39 (2008) 1747–1757.
 [26] G.A. Lu, C.Y. Wang, T.J. Yeh, Z. Zhang, *Electrochim. Acta* 49 (2004) 821–828.
 [27] Y. Cha, H.-G. Choi, J.-D. Nam, Y. Lee, S. ", H.-Y. Cha, H.-G. Choi, J.-D. nam, Y. Lee, S.M. Cho, E.-S. Lee, J.-K. Lee, C.-H. Chung, *Electrochim. Acta* 50 (2004) 795–799.
 [28] S.-C. Yao, X. Tang, C.-C. Hsieh, Y. Alyousef, M. Vladimer, G.K. Fedder, C.H. Amon, *Energy* 31 (2006) 636–649.
 [29] Y. Zhang, J. Lu, S. Shimano, H. Zhou, R. Maeda, *Electrochem. Commun.* 9 (2007) 1365–1368.
 [30] S.W. Lim, S.W. Kim, H.J. Kim, J.E. Ahn, H.S. Han, Y.G. Shul, *J. Power Sources* 161 (2006) 27–33.
 [31] J.-W. Guo, X.-F. Xie, J.-H. Wang, Y.-M. Shang, *Electrochim. Acta* 53 (2008) 3056–3064.
 [32] R. O'Hayre, S.-W. Cha, W. Colella, F.B. Prinz, *Fuel Cell Fundamentals*, John Wiley & Sons, New York, 2006.